



HAL
open science

The ecology of modern and fossil vertebrates revisited by lithium isotopes

Fanny Thibon, Jean Goedert, Nicolas Séon, Lucas Weppe, Jeremy E Martin,
Romain Amiot, Sylvain Adnet, Olivier Lambert, Paco Bustamante,
Christophe Lécuyer, et al.

► To cite this version:

Fanny Thibon, Jean Goedert, Nicolas Séon, Lucas Weppe, Jeremy E Martin, et al.. The ecology of modern and fossil vertebrates revisited by lithium isotopes. *Earth and Planetary Science Letters*, 2022, 599, pp.117840. 10.1016/j.epsl.2022.117840 . hal-03819112

HAL Id: hal-03819112

<https://hal.science/hal-03819112>

Submitted on 18 Oct 2022

HAL is a multi-disciplinary open access archive for the deposit and dissemination of scientific research documents, whether they are published or not. The documents may come from teaching and research institutions in France or abroad, or from public or private research centers.

L'archive ouverte pluridisciplinaire **HAL**, est destinée au dépôt et à la diffusion de documents scientifiques de niveau recherche, publiés ou non, émanant des établissements d'enseignement et de recherche français ou étrangers, des laboratoires publics ou privés.

1 The ecology of modern and fossil vertebrates revisited by lithium
2 isotopes

3

4 Fanny Thibon^{1*}, Jean Goedert², Nicolas Séon², Lucas Weppe^{1,3}, Jeremy E. Martin⁴, Romain
5 Amiot⁴, Sylvain Adnet⁵, Olivier Lambert⁶, Paco Bustamante^{3,7}, Christophe Lécuyer⁴, Nathalie
6 Vigier¹

7

8 ¹Laboratoire d'Océanographie de Villefranche-sur-Mer (LOV), CNRS UMR 7093/Sorbonne
9 Université; 06230 Villefranche-sur-Mer, France.

10 ²Muséum National d'Histoire Naturelle (MNHN) - Centre de Recherche en Paléontologie – Paris
11 (CR2P), CNRS UMR 7207/Sorbonne Université; 75231 Paris Cedex 05, France.

12 ³Littoral Environnement et Sociétés (LIENSs), CNRS UMR 7266/La Rochelle Université; F-17000
13 La Rochelle, France.

14 ⁴Laboratoire de Géologie de Lyon, Terre, Planètes et Environnement (LGL-TPE), Université
15 Claude Bernard Lyon1/CNRS UMR 5276/École Normale Supérieure de Lyon; 69622 Villeurbanne
16 Cedex, France.

17 ⁵Institut des Sciences de l'Evolution de Montpellier (ISEM) – Université de Montpellier/CNRS
18 UMR 5554/IRD/Ecole Pratique des Hautes Etudes; 34095 Montpellier Cedex 5, France.

19 ⁶Direction Opérationnelle Terre et Histoire de la Vie, Institut Royal des Sciences Naturelles de
20 Belgique; 1000 Brussels, Belgium.

21 ⁷Institut Universitaire de France (IUF); 75005 Paris, France.

22

23 *Corresponding author: Fanny Thibon

24 **Email:** thibon.fanny@orange.fr

25 **Abstract**

26 The vertebrate fossil record documents a plethora of transitions between aquatic and terrestrial
27 environments but their causes are still debated. Quantifying the salinity of living environments is
28 therefore crucial for precisising the sequence of ecological transitions. Here, we measured lithium
29 stable isotope composition of mineralized tissues ($\delta^7\text{Li}_{\text{mt}}$) of extant and extinct vertebrates from
30 various aquatic environments: seawater, freshwater/terrestrial, and "transitional environments"
31 (i.e. brackish waters, or seasonal access to freshwater and seawater). We report statistically
32 higher $\delta^7\text{Li}_{\text{mt}}$ values for seawater vertebrates than freshwater ones, taxonomic groups considered
33 separately. Moreover, vertebrates living in transitional environments have intermediate $\delta^7\text{Li}_{\text{mt}}$
34 values. Therefore, we show that $\delta^7\text{Li}_{\text{mt}}$ values of both extant and extinct vertebrates can
35 discriminate their aquatic habitat.

36

37 **Keywords:** Lithium isotopes – Mineralized tissues – Aquatic environments – Paleoecology

38 **1. Introduction**

39 Vertebrate species can face variable water environments during their lifetime. As salinity varies
40 drastically between marine waters and freshwater/terrestrial environments, it is a key parameter
41 for vertebrates (Gutiérrez, 2014). However, these environmental shifts remain challenging and
42 important to trace, notably to understand the cryptic life of modern aquatic vertebrate species,
43 especially fish (Maxwell, 2007; Mesiar et al., 1990), or to shed light on the evolution of past
44 aquatic vertebrate. Indeed, the aquatic vs terrestrial environmental dichotomy was pivotal during
45 the evolution of life on Earth (Pyenson et al., 2014; Uhen, 2007), and vertebrates have adapted to
46 salinity variations through complex morphological and physiological changes. It is therefore
47 crucial to possess tools to characterize the aquatic habitat of current and past vertebrate species.

48 To this end, stable isotopes are commonly used as modern and past ecological proxies (Fry,
49 2006). They are notably applied to vertebrate mineralized tissues (bones, teeth, eggshells,
50 scales, fish otoliths) to investigate current to past biological and physiological characteristics such
51 as body temperature (Amiot et al., 2006; Séon et al., 2020), mobility (Fricke et al., 2009; Lazzerini
52 et al., 2021; Lugli et al., 2019), trophic ecology (Hassler et al., 2018; Wißing et al., 2019), and to
53 reconstruct living environments of ancient animals (Amiot et al., 2010; Goedert et al., 2020,
54 2018).

55 In recent decades, stable ($\delta^{13}\text{C}$, $\delta^{18}\text{O}$, $\delta^{34}\text{S}$) and radiogenic isotope systems ($^{87}\text{Sr}/^{86}\text{Sr}$) applied to
56 vertebrate mineralized tissues have proved to be the best relevant palaeoecological proxies for
57 reconstructing salinity and/or the environmental conditions of their aquatic environments (i.e.
58 seawater vs freshwater) (Clementz et al., 2006; Fischer et al., 2012; Goedert et al., 2020, 2018;
59 Kocsis et al., 2009; Schmitz et al., 1997). However, they also hold limitations. First, post-
60 depositional diagenetic processes may affect the pristine isotopic composition of vertebrate
61 mineralized tissues through element absorption or dissolution by contact between earth fluids and
62 bioapatite. It is, however, worth noting that bone is more prone to extensive alteration than tooth
63 enamel, which is resistant to dissolution-recrystallization processes as shown experimentally by
64 Zazzo *et al.* (Zazzo et al., 2004). In parallel, some environmental estimations remain debated due

65 to other constraints of these isotopic proxies. Among them: (i) C and O are major elements
66 essential to life and numerous biological processes can affect their isotopic distributions (Fry,
67 2006); (ii) $\delta^{18}\text{O}$ is a poor proxy of salinity at low latitude (Dansgaard, 1964); (iii) a weak marine
68 influence can overshadow the continental signal recorded in bone $\delta^{34}\text{S}$ (Goedert et al., 2018);
69 and (iv) $^{87}\text{Sr}/^{86}\text{Sr}$ values of terrestrial vertebrates can be mistaken as marine values depending on
70 the type of bedrock inhabited (Holt et al., 2021); (v) significant overlap in $\delta^{13}\text{C}$ values may occur
71 between marine vertebrates and terrestrial ones consuming C4 vegetation (e.g. Clementz et al.,
72 2006). Furthermore, species migrating between waters of different salinities or living in brackish
73 waters can have $\delta^{18}\text{O}$ or $\delta^{34}\text{S}$ signatures indistinguishable from species living in seawater
74 (Goedert et al., 2020). Only the joint application of these two isotopic systems might overcome
75 such potential bias, as two recent studies indicate (Goedert et al., 2020, 2018).

76 We address these challenges of assessing the aquatic environments of both modern and extinct
77 vertebrate species by using a new stable isotopic proxy: lithium (Li). Unlike C and S, Li is not a
78 nutrient. Lithium also displays a broader range of isotope fractionation than C and O (Fanny
79 Thibon et al., 2021). Therefore, the Li stable isotope system presents a clear-cut advantage in
80 distinguishing aquatic environments based on salinity differences. Earth's rocks reservoirs have
81 $\delta^7\text{Li}$ values that vary among various environments (Penniston-Dorland et al., 2017), from -15 to
82 +20 ‰. Dissolved Li concentration and isotope composition in freshwaters (lakes, groundwaters,
83 rivers) display significant variations, from 0.1 to 22 ng/mL in concentration, and from +1 to +44 ‰
84 in $\delta^7\text{Li}$ values (Huh et al., 1998). In addition, due to its weak capacity to adsorb onto marine
85 particles (Decarreau et al., 2012), seawater Li mainly exists under free Li^+ ions forming stable
86 complexes with four water molecules (Rempe et al., 2018; Rudolph et al., 1995). Since dissolved
87 Li has a long oceanic residence time (~1.2 million years (Lécuyer, 2016)) far greater than the
88 ocean mixing time, it is homogeneously distributed throughout the water column (Misra and
89 Froelich, 2012) and between the oceans, which have both a constant Li concentration of 179
90 ng/mL (Broecker and Peng, 1982) and a $\delta^7\text{Li}$ value of $+31.0 \pm 0.5$ ‰ (Millot et al., 2004). Based
91 on recent palaeoceanographic reconstructions, seawater $\delta^7\text{Li}$ values remained constant during

92 the last 10 Ma, and progressively decreased to 22 ‰ 65 Ma ago (Misra and Froelich, 2012).
93 Here, we report the first measured Li stable isotope compositions of vertebrate mineralized
94 tissues ($\delta^7\text{Li}_{\text{mt}}$; bones and teeth) from 74 modern and 11 fossil specimens inhabiting different
95 types of environments (terrestrial, semi-aquatic, aquatic) and relying on either freshwater or
96 seawater.

97

98 **2. Materials and Methods**

99 2.1. Sampling and sample preparation

100 74 modern and 11 fossil bones and teeth were sampled from 5 taxonomic groups, namely
101 Chondrichthyes, Osteichthyes, Mammalia, Reptilia, and Amphibia.

102 2.1.1. Modern samples

103 Amphibian vertebrae (samples Pe-ri-1–5) were all collected from a breeding farm in Pierrelatte
104 (Drôme, France). Freshwater fish vertebrae (samples Si-gl-1 and Cy-Ca-1) were collected from a
105 lake in the Dombes region (Ain, France), operated by Maison Liatout. The majority of seawater
106 fish vertebrae (samples Di-la-1, So-so-1, Li-li-1, Li li 2, Li-li-3, Ga-mo-1, Ga-mo-2, On-ne-1, Mu-
107 su-1, Mu-su-2, Se-ma-1, Se-ma-2, Sp-au-1, Pl-pl-1, Di-la-2, Pa-pa-1, Sp-ca-1, Sa-sa-1, XG33
108 and TT3) were collected from fisheries and come from different locations specified in Table S1.
109 The majority of Mammalia and Reptilia samples (bone powder collected from different parts of the
110 skeleton, cf. Table S1, samples 50.001461, 50.001410, 50.001331, 50.001018, 50.001014,
111 50.001020, 50.001027, 50.001023, 50.002521, 50.000517, 50.002365, 50.001353, 50.001313,
112 50.000229, 50.001036, 50.001046, 50.000527, 50.001682, 50.001681, 50.002123, 50.002041,
113 50.002038, 50.002039, 50.000788) come from the collection of the Musée des Confluences
114 (Lyon, France). Additional Mammalia vertebrae (CC6, DD3, MDD1, PV8) and tooth bulk (samples
115 DD29, DD46, MDD36, PV42) were sampled from stranding specimens collected by PELAGIS
116 and the Museum National d'Histoire Naturelle (MNHN, Paris, France). Two Mammalia bone
117 fragment samples (JM18031 and JM1536) were collected from skeletons at the Institut Royal des

118 Sciences Naturelles de Belgique (IRSNB, Brussels, Belgium). The two samples of Mammalia
119 dentine (JM1502B and Inia) were collected from the IRSNB and the Naturhistorisches Museum
120 Basel (Switzerland) (sample N° 7167), respectively. The Chondrichthyes tooth bulk (REC0321M,
121 REC0204M, REC0610M, REC0270M, REC 767, REC 592M, REC 706-711, REC 1570M and
122 REC 1571M) are collection specimens from the Institut des Sciences de l'Évolution, Montpellier
123 (ISEM), University of Montpellier, France.

124 2.1.2.Fossil samples

125 All the fossil samples (1-BAZ-19, 1-BAZ-23, 1-BAZ-8e, 1-BAZ-8d, 1-BAZ-17e, 1-BAZ-17d, 1-
126 BAZ-4e, 1-BAZ-4d, 1-BAZ-14e, 1-BAZ-16e, 1-BAZ-16d) were collected from Miocene deposits
127 that temporarily outcropped in the municipality of Bazas (Aquitaine Basin, France). More details
128 are available in Goedert *et al.* (Goedert et al., 2017).

129 For all bone samples, we favored cortical bone. Bioapatite powder was collected either by
130 crushing bone and tooth samples into a fine powder using an agate mill or by using a Dremel™
131 equipped with a spherical diamond-tipped drill bit. Additional information (location, type of skeletal
132 material) is given for each sample in Table S1.

133 2.1.3.Chemical preparation

134 All analytical preparations were performed in a pressure-cleaned laboratory under a fume-hood to
135 minimize procedural blanks, using distilled reagents and pre-cleaned vessels. Approximately 5 to
136 10 mg of sample powder were first dissolved with a mixture of concentrated HNO₃ and H₂O₂.
137 After 48 h, concentrated HCl was added to pursue the digestion in inverse aqua regia, and
138 heated for 24 h before being evaporated.

139 Lithium extraction and purification were performed following a well-documented routine procedure
140 (James and Palmer, 2000; Vigier et al., 2009), recently adapted to biological materials and
141 tissues (Thibon et al., 2021). Samples were taken up in 0.5 mL of 1 N HCl and loaded on AG 50-
142 X12 (200-400 mesh) resin in 8.5-cm-high Teflon columns. Lithium was eluted with 1 N HCl. A

143 second purification step, following the same procedure as the first Li extraction, ensured complete
144 separation of Li.

145 Five total procedural blanks and five replicates of cow bone ash reference material (SRM-1400)
146 were included. The precision and accuracy of the overall procedure were checked and published
147 in Thibon *et al.* (Fanny Thibon et al., 2021).

148 2.2. Analytical measurements

149 Lithium has two naturally occurring isotopes (${}^7\text{Li}$ - ${}^6\text{Li}$). The isotopic compositions of geological
150 and biological materials are reported as per-mil variations relative to an isotopic standard (here
151 NIST L-SVEC-1 SRM 8545) as $\delta^7\text{Li}_{\text{sample}} [\text{‰}] = (({}^7\text{Li}/{}^6\text{Li})_{\text{sample}} / ({}^7\text{Li}/{}^6\text{Li})_{\text{LSVEC}} - 1) \times 1,000$. Li
152 isotopic analyses were performed using a Thermo-Fisher Neptune Plus multi-collector inductively
153 coupled plasma mass spectrometer (LGL-TPE UMR CNRS 5276, France) following the
154 procedure developed for low Li concentrations in biological materials (Balter and Vigier, 2014;
155 Bastian et al., 2018; Fanny Thibon et al., 2021). Samples and standards were analyzed under dry
156 plasma conditions in low-resolution mode. The standard bracketing method (using the LSVEC
157 reference material) was used to performed instrumental mass bias correction. The five total Li
158 procedural blanks, which included chemical and analytical blanks, ranged between 20 and 40 pg.
159 For 10 mg of material with a Li concentration of 1 $\mu\text{g/g}$, the maximum blank contribution was
160 negligible (0.4 ‰). On average, the internal reproducibility was ± 0.04 ‰. Precision (external
161 reproducibility) was estimated from 2 to 6 replicate measurements of 29 different samples, and
162 ranged from 0.1 to 0.9 ‰ (2SD). Cow bone ash reference material (SRM-1400), previously
163 published at -1.7 ± 0.1 ‰ (2SE) (Fanny Thibon et al., 2021), was measured here at -1.9 ± 0.3 ‰
164 (2SE, $n = 5$), which confirmed the procedure's accuracy. Li concentrations have been estimated
165 using voltage measurements during isotopic measurements (using a normalization to a LSVEC
166 calibrated solution).

167 2.3. Body mass estimation

168 We additionally reported the body mass for Chondrichthyes and Osteichthyes species (Tables
169 S1). When the body mass was not initially measured, but the total length was, we used length-
170 weight relationships: (LWR) $\text{weight} = a(\text{total length})^b$ (Froese et al., 2014), with the LWR
171 parameters a and b taken from www.fishbase.org.

172 2.4. Statistical treatments

173 Since normality and homoscedasticity of the Li isotopic data were not validated, the non-
174 parametric Mann-Whitney-Wilcoxon and Kruskal-Wallis tests were used to compare median
175 values between two or more observational series, respectively. Tests were performed using R
176 software (R Core Team, 2017) using the functions *wilcox.test* or *kruskal.test*. The level of
177 significance for statistical analyses was set at $p\text{-val} < 0.05$.

178 A linear model was used to decipher which factors play a key role in the Li isotope compositions.
179 The predictors applied to the model are the body mass, trophic levels, Li concentrations,
180 taxonomic group, water mode (seawater/freshwater/intermediate water), and life mode
181 (aquatic/semi-aquatic/terrestrial).

182

183 3. Results and Discussion

184 According to the linear model, only 3 variables are significant predictors: water and life modes (p -
185 val < 0.001), and taxonomic group (p -val < 0.05). The following sections, therefore, focus on
186 these variables.

187 3.1. Characterizing aquatic environments using $\delta^7\text{Li}_{\text{mt}}$

188 $\delta^7\text{Li}_{\text{mt}}$ values of modern aquatic and terrestrial vertebrates cover an extensive range, from -24.0
189 to +36.0 ‰. While their Li concentrations are relatively low, they also vary considerably, from 0.1
190 to 6.3 $\mu\text{g/g}$ dry weight (Fig. S1 and Table S1). Considering taxonomic groups separately,
191 vertebrates living in seawater have, on average, significantly higher $\delta^7\text{Li}_{\text{mt}}$ values (26.8 ± 6.8 ‰
192 (SD, $n=7$), 16.5 ± 3.4 ‰ (SD, $n=13$), 9.0 ± 5.6 ‰ (SD, $n=20$) for Chondrichthyes, Osteichthyes

193 and Mammalia, respectively) than those in freshwater ($-2.8 \pm 3.0 \text{ ‰}$ (SD, n=2), $-5.0 \pm 4.6 \text{ ‰}$ (SD,
194 n=2), $-9.0 \pm 7.4 \text{ ‰}$ (SD, n=9) for Chondrichthyes, Osteichthyes and Mammalia, respectively;
195 Wilcox. test, $p\text{-val} < 0.05$, < 0.05 , and < 0.0001 , respectively; Figs. 1 and 2, Table 1). However, Li
196 concentrations of mineralized tissues are not significantly different between vertebrates living in
197 seawater and freshwater ($1.0 \pm 0.6 \text{ } \mu\text{g/g}$ (SD, n=20) vs. $0.5 \pm 0.3 \text{ } \mu\text{g/g}$ (SD, n=9) for Mammalia
198 living in seawater and freshwater; Wilcox. test, $p\text{-val} > 0.05$), except for Chondrichthyes and
199 Osteichthyes ($2.0 \pm 0.7 \text{ } \mu\text{g/g}$ (SD, n=7) and $2.0 \pm 0.9 \text{ } \mu\text{g/g}$ (SD, n=13), for Chondrichthyes and
200 Osteichthyes living in seawater vs $0.4 \pm 0.2 \text{ } \mu\text{g/g}$ (SD, n=2) and $0.4 \pm 0.2 \text{ } \mu\text{g/g}$ (SD, n=2), and for
201 Chondrichthyes and Osteichthyes living in freshwater; Wilcox. test, $p\text{-val} < 0.05$, Figs. S1 and
202 S2).

203 The Li_{mt} concentrations and $\delta^7\text{Li}_{\text{mt}}$ values of bones from five marsh frogs (*Pelophylax ridibunda*),
204 raised in the same basin and sharing the same water and food resources, are homogenous and
205 vary from $0.36 \text{ } \mu\text{g/g}$ to $0.53 \text{ } \mu\text{g/g}$ with a mean of $0.46 \pm 0.06 \text{ } \mu\text{g/g}$ (SD, n = 5), and from -12.9 ‰ to
206 -7.6 ‰ with a mean of $-9.6 \text{ ‰} \pm 2.1 \text{ ‰}$ (SD, n = 5), respectively. The same comparisons cannot
207 be made with teeth since teeth from different individuals of the same species living in similar
208 environments were not sampled in this study. As for bone and tooth samples from single
209 individuals, distinct Li_{mt} concentrations and $\delta^7\text{Li}_{\text{mt}}$ values were recorded, showing tooth-bone
210 differences ranging from $0.2 \text{ } \mu\text{g/g}$, for the harbour seal (*Phoca vitulina*) to $1.7 \text{ } \mu\text{g/g}$ for the short-
211 beaked common dolphin (*Delphinus delphis*), and from -2.5 ‰ for the short-beaked common
212 dolphin to $+10.1 \text{ ‰}$ for the harbour seal (Table S2). Nevertheless, these differences fell within
213 value ranges corresponding to the same aquatic environmental condition. Both inter- and intra-
214 individual $\delta^7\text{Li}_{\text{mt}}$ value variabilities potentially result from isotopic fractionations during biological
215 and physiological processes. As reported by Poet, Vigier, Bouret et al. (submitted to iScience), Li
216 isotopes are strongly fractionated by cell transporters, and therefore may lead to variable isotopic
217 compositions between organs (tooth vs. bones) and between individuals from the same species.
218 These isotopic effects were also detected in mussels cultured under various conditions (Thibon et
219 al., 2021). Nevertheless, these variabilities do not overprint the environmental variability. Indeed,

220 $\delta^7\text{Li}_{\text{mt}}$ values can distinguish between Osteichthyes living in seawater, freshwater, and
221 "transitional environments", i.e. brackish waters, or seasonally crossing waters of different
222 salinities, such as the sockeye salmon (*Onchorynchus nerka*) (Figs. 1 and 2, $\delta^7\text{Li}_{\text{mt}}$ values being
223 $+16.5 \pm 3.4 \text{ ‰}$ (SD, n=13), $+9.9 \pm 2.9 \text{ ‰}$ (SD, n=8), and $-5.0 \pm 4.6 \text{ ‰}$ (SD, n=2), respectively for
224 fish living in seawater, transitional environments, and freshwater). $\delta^7\text{Li}_{\text{mt}}$ values of fish species
225 living in transitional environments are intermediate and statistically different from $\delta^7\text{Li}_{\text{mt}}$ values of
226 fish living in seawater and freshwater (Wilcox. test, $p\text{-val} < 0.05$ and < 0.0001 , respectively, Fig.
227 2). Furthermore, the Li concentrations of their mineralized tissues (Li_{mt}) also reflect their living
228 environment since Osteichthyes Li_{mt} values are statistically different between seawater,
229 freshwater, and transitional environments (respectively $2.0 \pm 0.9 \mu\text{g/g}$ (SD, n=13), $0.4 \pm 0.2 \mu\text{g/g}$
230 (SD, n=2), $1.4 \pm 0.4 \mu\text{g/g}$ (SD, n=8), Wilcox. test, $p\text{-val} < 0.05$, Fig. S2). Consequently, both $\delta^7\text{Li}_{\text{mt}}$
231 values and Li concentrations allow clear discrimination between seawater/transitional/freshwater
232 groups (Fig. S6). Water salinity thus has a noticeable effect on Li accumulation, transport, and/or
233 excretion in vertebrate mineralized tissues. In contrast, O and S isotopes need to be considered
234 jointly to distinguish fish species living in transitional environments (Goedert et al., 2020, 2018)
235 (Figs. 3a and 3b). The Li entry in biological cells can explain its isotope variability between
236 environments of different salinity. Indeed, the two major ions that influence salinity are chloride
237 and sodium, although salinity is based on a large diversity of elements. Lithium can enter
238 biological cells through Na/H exchangers (NHE) following Na ions (Counillon et al., 2016). The
239 competition between Li and Na leads to Li isotope fractionation that varies according to water
240 Li/Na ratio, up to $\sim 13 \text{ ‰}$ in favor of the light isotope ^6Li (Poet et al., submitted to iScience). Li
241 bioaccumulation may also be different in Li-rich (seawater) and Li-poor (river waters)
242 environments, and this may also affect Li isotope composition of biological tissues (Thibon et al.,
243 2021).

244 The first straightforward application of Li stable isotope compositions in vertebrate mineralized
245 tissues concerns modern ecology. Numerous fish species spend time in both marine and
246 freshwater environments throughout their lifetime (Jones, 2006; Quinn, 2018). Furthermore, many

247 species inhabiting transitional environments, such as estuaries, are spatially distributed along a
248 salinity gradient (Jones, 2006). These habitats are difficult to establish solely from visual
249 observation of collected specimens. Indeed, routine monitoring techniques, such as acoustic or
250 satellite telemetry through physical tracking (Hussey et al., 2015), or hydroacoustic surveys
251 (Maxwell, 2007; Mesiar et al., 1990), encounter obstacles when following species that are highly
252 mobile, undertake large-scale migrations, or have high migrant numbers. Due to the broad
253 variability of $\delta^7\text{Li}_{\text{mt}}$ values in the environment and the clear distinction between marine and
254 freshwater/terrestrial environments, Li stable isotopes are useful for elucidating living
255 environments. In addition, stable isotope compositions such as $\delta^{13}\text{C}$, $\delta^{15}\text{N}$ or $\delta^{34}\text{S}$, while being
256 powerful tools for identifying and characterizing environmental niches of fish species (Dwyer et
257 al., 2020; Fry and Chumchal, 2011) commonly rely on soft tissue such as muscles. Li stable
258 isotopes therefore offer an additional approach applicable to solid mineralized tissues of modern
259 fish, with $\delta^7\text{Li}_{\text{mt}}$ of paramount interest in transitional environments.

260

261 3.2. Biological imprints on the $\delta^7\text{Li}_{\text{mt}}$ record

262 Although $\delta^7\text{Li}_{\text{mt}}$ values reflect the living environments of modern species, they also display
263 important variations within a single environment. These variation ranges are of 19.7 ‰ (n = 7),
264 10.7 ‰ (n = 13), 22.0 ‰ (n = 20), and 10.1 ‰ (n = 3) for modern seawater Chondrichthyes,
265 Osteichthyes, Mammalia, and Reptilia, respectively, and 4.3 ‰ (n = 2), 6.5 ‰ (n = 2), 22.3 ‰ (n
266 = 9) and 6.3 ‰ (n = 4) for modern freshwater counterparts. Yet, these variations do not mask the
267 influence of the environment, especially for Chondrichthyes and Osteichthyes, since no overlaps
268 in $\delta^7\text{Li}_{\text{mt}}$ values are reported in the present dataset (Figs. 1 and 2). We thus investigated
269 biological parameters that could affect $\delta^7\text{Li}_{\text{mt}}$ values from the same taxonomic group within similar
270 environments and also explain differences in values between two taxonomic groups inhabiting
271 similar environments.

272 First of all, as lithium is effectively incorporated in marine species by filtration and by predation
273 (Thibon et al., 2020), the quantity of filtrated water may impact both Li concentration and isotopic
274 composition of Chondrichthyes and Osteichthyes biological mineralized tissues. The amount of
275 filtrated water directly depends on the gill surface area, which is linked to the body mass (Bigman
276 et al., 2018). A positive relationship between $\delta^7\text{Li}_{\text{mt}}$ values and body mass is highlighted in Fig. 4
277 ($r = 0.69$, $p\text{-val} < 0.001$). In this way, a metabolic effect may affect $\delta^7\text{Li}_{\text{mt}}$ values. As mentioned
278 above, Li can enter biological cells through NHE (Counillon et al., 2016). The latter can
279 fractionate Li isotopes in favor of the light isotope ^6Li (Poet et al., submitted to iScience. As for
280 isotopic fractionation occurring during Rayleigh distillation, it seems that the more water that is
281 filtrated, the more Li passing through gill cell NHE, but the less Li isotopically fractionated with
282 respect to seawater. This could explain why the heavier Chondrichthyes displays $\delta^7\text{Li}_{\text{mt}}$ values
283 close to seawater's, and the smaller Osteichthyes, much lower values (Fig. 4). Furthermore, this
284 can also explain the proximity of $\delta^7\text{Li}_{\text{mt}}$ values between Osteichthyes and Chondrichthyes of close
285 body mass (Figs. 1 and 4). However, this hypothesis must be further investigated due to
286 differences between Osteichthyes and Chondrichthyes gill anatomy and physiology (Evans et al.,
287 2005).

288 On average, cetaceans living in seawater have $\delta^7\text{Li}_{\text{mt}}$ values lower than marine Osteichthyes or
289 Chondrichthyes (respectively $+12.3 \pm 4.4$ ‰ (SD, $n=10$), $+16.5 \pm 3.4$ ‰ (SD, $n=13$), $+26.8 \pm 6.8$
290 ‰ (SD, $n=7$), Fig. 1, $p\text{-val} < 0.05$). Significantly, their principal Li source, differently from
291 Osteichthyes and Chondrichthyes, is food ingestion. This suggests that, secondarily to filtration,
292 supplementary biological mechanisms fractionate Li stable isotopes during intestinal assimilation,
293 ultimately favoring the relative incorporation of ^6Li in bones.

294 Meanwhile, terrestrial vertebrates such as mammals have lower $\delta^7\text{Li}_{\text{mt}}$ values than semi-aquatic
295 or aquatic freshwater mammals, except for the Amazon river dolphin (*Inia geoffrensis*). This is
296 also the case for terrestrial and semi-aquatic birds originating from the same geographic area
297 (Fig. 1). This tendency hints at potential fractionation mechanisms in terrestrial environments
298 resulting in relative concentration of the lighter isotope (^6Li) in mineralized tissues.

299 It is worth noting that $\delta^7\text{Li}_{\text{mt}}$ values are also valuable for tracking the feeding habits of vertebrates.
300 For instance, the polar bear (*Ursus maritimus*) and the sea otter (*Enhydra lutris*) have $\delta^7\text{Li}_{\text{mt}}$
301 values of +11.3 ‰ and + 8.03 ‰, respectively, which fall within the range of seawater aquatic
302 mammal values. Although terrestrial species rely on freshwater for their water supply, polar bears
303 and sea otters feed on marine aquatic species such as seals or molluscs, hence their $\delta^7\text{Li}_{\text{mt}}$
304 values. In modern ecology, $\delta^7\text{Li}_{\text{mt}}$ values thus represent a reliable tool to test marine resource
305 uptake in terrestrial species (Bicknell et al., 2020).

306

307 3.3. Palaeoecological implications

308 Overall, $\delta^7\text{Li}_{\text{mt}}$ values of Miocene fossil vertebrates from the Aquitaine Basin (France) are
309 consistent with observed modern $\delta^7\text{Li}_{\text{mt}}$ values and clearly discriminate between marine and
310 freshwater vertebrate taxa (Fig. 1). All fossil $\delta^7\text{Li}_{\text{mt}}$ values fall within the seawater/freshwater
311 ranges defined by the present-day samples, apart for the dentine sample of the terrestrial
312 mammal *Gomphotherium angustidens*, and agree with stable oxygen isotope compositions from
313 a previous study (Goedert et al., 2017). Of particular note, the highest fish $\delta^7\text{Li}_{\text{mt}}$ value,
314 corresponding to the fossil fish *Trigonodon jugleri*, falls within the range of modern seawater fish.
315 This may be linked to the specimen's size. Indeed, even though its modern counterparts
316 (*Pseudodax moluccanus*) measure approximately 25 cm, Miocene *T. jugleri* tooth size indicates a
317 body length of about 1 meter, assuming isometry (Schultz and Bellwood, 2004), making it
318 comparable to the largest modern marine fish we sampled, namely the Bluefin tuna (*Thunnus*
319 *thynnus*). As discussed in previous sections, filtration through the gills may explain this extreme
320 value, and supports a larger specimen size as suggested by Schultz & Bellwood (Schultz and
321 Bellwood, 2004).

322 A body size effect on Li isotope compositions is however ruled out for the fossil Chondrichthyes
323 *Otodus megalodon* and *Cosmopolitodus hastalis* — large species with slightly lower $\delta^7\text{Li}_{\text{mt}}$ values
324 than their modern seawater counterpart. *O. megalodon* spatial distribution was wide: nurseries

325 have been found in shallow waters while adults lived in the open ocean far from coasts (Pimiento
326 et al., 2010). Furthermore, these sharks inhabited waters with annual mean temperatures from 12
327 to 27 °C (Pimiento et al., 2016). Indeed, they could efficiently regulate their body temperature,
328 allowing them to dwell in cold waters (Pimiento et al., 2016). In addition, they may have
329 frequented in deep waters like their modern analogue, the great white shark (Pimiento et al.,
330 2016), which can dive as deep as 1000 m (Skomal et al., 2017). Therefore, their habitat may
331 have had different salinity ranges than modern sharks, and additional biological factors could
332 have influenced their Li isotopic signatures.

333 As for sirenians, both seawater subfossil Steller's sea cow (*Hydrodamalis gigas*) and modern
334 dugong (*Dugong dugon*) samples display $\delta^7\text{Li}$ values close to those of the fossil Dugongidae
335 (+3.7, +7.7, +6.7 vs +5.2 ‰, respectively, see Fig. 1 and Table S2). This supports the notion that
336 after mammals recolonized aquatic environments in the Eocene (cetaceans and sirenians), some
337 species (Miocene Dugongidae) stayed in seawater environments while others, such as some
338 Trichechinae, recolonized freshwater environments (Suarez et al., 2021).

339 In contrast to traditional isotopic systems (C, O, S, Sr), there is little insight on the behavior of Li
340 in apatite during fossilization processes. Important shifts can be expected if recrystallization of
341 secondary minerals occurs in a diagenetic fluid impacted, for example, by clay dissolution (rich in
342 Li, and with low $\delta^7\text{Li}$ compared to waters). Nevertheless, in fossil carbonates (i.e., foraminifera), it
343 has already been shown that certain early diagenetic histories have a negligible influence on Li
344 isotopes (Misra and Froelich, 2012). We can therefore expect good signal preservation in
345 apatites, a mineral that is thermodynamically more stable than carbonates. Here, we observe no
346 clear relationship between fossil $\delta^7\text{Li}_{\text{mt}}$ values and Li concentrations ($p\text{-val} > 0.05$, Fig. S3),
347 suggesting a negligible effect of diagenesis on Li and $\delta^7\text{Li}$. Furthermore, no significant correlation
348 is observed between $\delta^7\text{Li}_{\text{mt}}$ values or Li_{mt} and elements classically used as diagenesis proxies,
349 such as Rare Earth Elements, data previously published in Goedert *et al.* (Goedert et al., 2017)
350 ($R^2 = 0.04$ and 0.19 , respectively; $p\text{-val} > 0.05$; Fig. S4). Nevertheless, fossil dentine and enamel
351 from *O. megalodon* and Rhinocerotidae have similar $\delta^7\text{Li}_{\text{mt}}$ values (+14.8 vs +14.6 ‰ and -1.4 vs

352 -1.7 ‰, respectively, Fig. S5 and Table S2). This, however, is not the case of *C. hastalis* and *G.*
353 *angustidens* (+13.9 vs +21.9 ‰ and +8.0 vs -5.0 ‰, respectively, Fig. S5 and Table S2). Being
354 more porous than enamel, dentine is more prone to chemical alterations during diagenesis.
355 Indeed, Li is highly mobile in aqueous fluids, and may be lost from dentine during diagenesis,
356 altering the pristine Li isotope composition. However, almost all fossil vertebrate samples have
357 higher Li concentrations than their present-day counterparts (Fig. S1 and Table 1). Therefore,
358 either a Li gain took place during diagenesis without deeply affecting the isotopic composition, or
359 environmental Li concentrations were higher in the past or at least in this specific
360 paleoenvironmental context. It should be noted that systematic Li gain during diagenesis is not
361 expected due to Li incompatibility with apatite (Brophy et al., 2011; Penniston-Dorland et al.,
362 2017). The second explanation is therefore more likely, considering that oceanic Li concentration
363 changed in the past (Misra and Froelich, 2012), and was potentially higher during the Burdigalian
364 (Hathorne and James, 2006). In addition, a higher oceanic Li concentration could have been
365 triggered by a higher Li river flux (Hathorne and James, 2006), thus also explaining the higher Li
366 environmental level for terrestrial fossils. All these hypotheses need further testing by additional
367 studies on both fossil and modern samples. Nevertheless, fossil data strongly support the
368 hypothesis that extinct vertebrate $\delta^7\text{Li}_{\text{mt}}$ values directly reflect the seawater/freshwater dichotomy
369 as present-day $\delta^7\text{Li}_{\text{mt}}$ values do.

370 Finally, in the field of archaeology, many studies investigate the foods items consumed by human
371 populations (Ambrose and DeNiro, 1986). One recurrent question concerning the consumption of
372 marine vs terrestrial resources, especially among populations living near coastal areas, is
373 currently addressed by stable isotope compositions such as $\delta^{15}\text{N}$ or $\delta^{34}\text{S}$ (Lécuyer et al., 2021).
374 As discussed in section 3.2, $\delta^7\text{Li}_{\text{mt}}$ values may also be valuable for tracking the feeding habits of
375 vertebrates. Here again, Li has the potential to become powerful for detecting the consumption of
376 marine resources by terrestrial vertebrates.

377 Another advantage Li isotopes in mineralized tissues bring to paleo-ecological questions is that
378 soft tissues from deep times (> 1 Ma) have disappeared, leaving only mineralized tissues in

379 sediments, namely an abundance of vertebrate bones, teeth, or fish scales in the fossil record.
380 According to this preliminary study, at least part of the pristine Li isotopic signature appears to be
381 preserved in enamel. Being more sensitive to transitional environments than oxygen or sulfur
382 isotopes, Li isotopes in fossil enamel of Devonian tetrapods, for example, may provide new clues
383 about their terrestrialization.

384

385 **4. Conclusions**

386 These results demonstrate that Li stable isotope compositions in bones and teeth from extant
387 vertebrate species constitute a valuable proxy for determining their aquatic environments, i.e.
388 seawater, freshwater, or transitional. Additional second-order variability might reflect biological
389 imprints such as the amount of water filtrated through fish gills. Moreover, Li isotopes in teeth and
390 bones might also benefit to the reconstruction of past environmental conditions using fossil
391 specimens. Although preliminary, the application of Li isotopes to fossil specimens already
392 underlines their potential, either for establishing biological features such as size/body mass in
393 relation to the quantity of filtrated water, as exemplified by *T. jugleri*, the habitat of *O. megalodon*
394 and *C. hastalis*, or the environmental conditions of aquatic habitat like for the fossil *Dugongidae*.
395 Overall, Li isotopes in mineralized tissues have the makings of a powerful tool for tracking the
396 ecology of past and present-day vertebrates. This new isotopic tool might benefit the fields of
397 ecology, archaeology and palaeontology by, respectively, tracking the living environments of
398 vertebrate species, determining whether past human populations relied on marine resources, and
399 resolving major past ecological transitions

400

401 **Acknowledgments**

402 Funding: Agence Nationale de la Recherche (ANR). Grant number: ANR-18-CE34-0002. Project
403 title: ISO2MET (www.iso2met-project.fr). We are grateful for access to facilities provided by the
404 Laboratoire Océanographique de Villefranche-sur-mer (LOV) and Laboratoire de Géologie de

405 Lyon, Terre-Planète-Environnement (LGL-TPE). JEM thanks L. Costeur (NHM Basel) for
406 permitting the sampling of *I. geoffrensis*. NS thanks F. Demaret (PELAGIS, UMS3462), W. Dabin
407 (PELAGIS, UMS3462) and C. Lefèvre (MNHN Paris) for permitting the sampling of bone and
408 tooth on several marine mammals. OL thanks O. Pauwels and S. Bruaux (IRSNB) for permitting
409 the sampling of bone and tooth on several marine mammals. FT and NV thank M. Montanes for
410 her management of the clean lab at LOV and F. Arnaud-Godet and P. Telouk for their help with
411 MC-ICP-MS at ENS Lyon. JG thanks the Musée des Confluences de Lyon and the curator M.
412 Berthet for providing access to skeletal material and for permission to sample specimens. The
413 IUF (Institut Universitaire de France) is acknowledged for its support to PB as a senior member.
414 We thank the editor and the two anonymous reviewers who helped improving this manuscript.

415

416 **Competing Interest Statement:** The authors declare no competing interests

417 **Data Availability:** All data underlying the study are in supplementary Data files (.xlsx format).

418

419 **Author Contributions:** CRediT author statement. F. **Thibon:** Conceptualization, Supervision,
420 Methodology, Validation, Investigation, Formal analysis, Visualization, Writing - original draft,
421 Writing - review & editing. J. **Goedert:** Conceptualization, Resources, Investigation, Writing -
422 review & editing. N. **Séon:** Resources, Investigation, Writing - review & editing. L. **Weppe:**
423 Methodology, Validation, Investigation, Writing – review & editing. J.E. **Martin:** Conceptualization,
424 Resources, Investigation, Writing - review & editing. R. **Amiot:** Resources, Investigation, Writing -
425 review & editing. S. **Adnet:** Resources, Investigation, Writing - review & editing. O. **Lambert:**
426 Resources, Investigation, Writing - review & editing. P. **Bustamante:** Funding acquisition, Writing
427 - review & editing. C. **Lécuyer:** Conceptualization, Investigation, Writing – review & editing. N.
428 **Vigier:** Resources, Funding acquisition, Investigation, Writing - review & editing.

429

430 **References**

431

432 Ambrose, S.H., DeNiro, M.J., 1986. Reconstruction of African human diet using bone collagen carbon and nitrogen
433 isotope ratios. *Nature* 319, 321–324. <https://doi.org/10.1038/319321a0>

434 Amiot, R., Buffetaut, E., Lécuyer, C., Wang, X., Boudad, L., Ding, Z., Fourel, F., Hutt, S., Martineau, F., Medeiros, M., Mo,
435 J., Simon, L., Suteethorn, V., Sweetman, S., Tong, H., Zhang, F., Zhou, Z., 2010. Oxygen isotope evidence for
436 semi-aquatic habits among spinosaurid theropods. *Geology* 38, 139–142. <https://doi.org/10.1130/G30402.1>

437 Amiot, R., Lécuyer, C., Buffetaut, E., Escarguel, G., Fluteau, F., Martineau, F., 2006. Oxygen isotopes from biogenic
438 apatites suggest widespread endothermy in Cretaceous dinosaurs. *Earth and Planetary Science Letters* 246,
439 41–54. <https://doi.org/10.1016/j.epsl.2006.04.018>

440 Balter, V., Vigier, N., 2014. Natural variations of lithium isotopes in a mammalian model. *Metallomics* 6, 582–586.

441 Bastian, L., Vigier, N., Reynaud, S., Kerros, M.-E., Revel, M., Bayon, G., 2018. Lithium Isotope Composition of Marine
442 Biogenic Carbonates and Related Reference Materials. *Geostandards and Geoanalytical Research* 42, 403–
443 415. <https://doi.org/10.1111/ggr.12218>

444 Bicknell, A.W.J., Walker, B.W., Black, T., Newton, J., Pemberton, J.M., Luxmoore, R., Inger, R., Votier, S.C., 2020. Stable
445 isotopes reveal the importance of seabirds and marine foods in the diet of St Kilda field mice. *Sci Rep* 10, 6088.
446 <https://doi.org/10.1038/s41598-020-62672-x>

447 Bigman, J.S., Pardo, S.A., Prinzing, T.S., Dando, M., Wegner, N.C., Dulvy, N.K., 2018. Ecological lifestyles and the
448 scaling of shark gill surface area. *Journal of Morphology* 279, 1716–1724. <https://doi.org/10.1002/jmor.20879>

449 Broecker, W.S., Peng, T.-H., 1982. *Tracers in the Sea*. Eldigio Press, Palisades, N.Y.

450 Brophy, J.G., Ota, T., Kunihro, T., Tsujimori, T., Nakamura, E., 2011. In situ ion-microprobe determination of trace
451 element partition coefficients for hornblende, plagioclase, orthopyroxene, and apatite in equilibrium with natural
452 rhyolitic glass, Little Glass Mountain Rhyolite, California. *American Mineralogist* 96, 1838–1850.
453 <https://doi.org/10.2138/am.2011.3857>

454 Clementz, M.T., Goswami, A., Gingerich, P.D., Koch, P.L., 2006. Isotopic records from early whales and sea cows:
455 contrasting patterns of ecological transition. *Journal of Vertebrate Paleontology* 26, 355–370.
456 [https://doi.org/10.1671/0272-4634\(2006\)26\[355:IRFEWA\]2.0.CO;2](https://doi.org/10.1671/0272-4634(2006)26[355:IRFEWA]2.0.CO;2)

457 Counillon, L., Bouret, Y., Marchiq, I., Pouyssegur, J., 2016. Na⁺/H⁺ antiporter (NHE1) and lactate/H⁺ symporters (MCTs) in
458 pH homeostasis and cancer metabolism. *Biochimica et Biophysica Acta (BBA)-Molecular Cell Research* 1863,
459 2465–2480. <https://doi.org/10.1016/j.bbamcr.2016.02.018>

460 Dansgaard, W., 1964. Stable isotopes in precipitation. *Tellus* 16, 436–468. <https://doi.org/10.1111/j.2153-3490.1964.tb00181.x>

461 Decarreau, A., Vigier, N., Pálková, H., Petit, S., Vieillard, P., Fontaine, C., 2012. Partitioning of lithium between smectite
462 and solution: An experimental approach. *Geochimica et Cosmochimica Acta* 85, 314–325.

463 Dwyer, R.G., Campbell, H.A., Cramp, R.L., Burke, C.L., Micheli-Campbell, M.A., Pillans, R.D., Lyon, B.J., Franklin, C.E.,
464 2020. Niche partitioning between river shark species is driven by seasonal fluctuations in environmental salinity.
465 *Functional Ecology* 34, 2170–2185. <https://doi.org/10.1111/1365-2435.13626>

466 Evans, D.H., Piermarini, P.M., Choe, K.P., 2005. The multifunctional fish gill: dominant site of gas exchange,
467 osmoregulation, acid-base regulation, and excretion of nitrogenous waste. *Physiol Rev* 85, 97–177.
468 <https://doi.org/10.1152/physrev.00050.2003>

469 Fischer, J., Voigt, S., Franz, M., Schneider, J.W., Joachimski, M.M., Tichomirowa, M., Götze, J., Furrer, H., 2012.
470 Palaeoenvironments of the late Triassic Rhaetian Sea: Implications from oxygen and strontium isotopes of
471 hybdont shark teeth. *Palaeogeography, Palaeoclimatology, Palaeoecology* 353–355, 60–72.
472 <https://doi.org/10.1016/j.palaeo.2012.07.002>

473 Fricke, H., Rogers, R., Gates, T., 2009. Hadrosaurid migration: Inferences based on stable isotope comparisons among
474 Late Cretaceous dinosaur localities. *Paleobiology* 35, 270–288. <https://doi.org/10.1666/08025.1>

475 Froese, R., Thorson, J.T., Reyes, R.B., 2014. A Bayesian approach for estimating length-weight relationships in fishes.
476 *Journal of Applied Ichthyology* 30, 78–85. <https://doi.org/10.1111/jai.12299>

477 Fry, B., 2006. *Stable Isotope Ecology*. Springer, New York.

478 Fry, B., Chumchal, M.M., 2011. Sulfur stable isotope indicators of residency in estuarine fish. *Limnology and*
479 *Oceanography* 56, 1563–1576. <https://doi.org/10.4319/lo.2011.56.5.1563>

480 Goedert, J., Amiot, R., Arnaud-Godet, F., Cuny, G., Fourel, F., Hernandez, J.-A., Pedreira-Segade, U., Lécuyer, C., 2017.
481 Miocene (Burdigalian) seawater and air temperatures estimated from the geochemistry of fossil remains from
482 the Aquitaine Basin, France. *Palaeogeography, Palaeoclimatology, Palaeoecology* 481, 14–28.
483 <https://doi.org/10.1016/j.palaeo.2017.04.024>

484 Goedert, J., Amiot, R., Berthet, D., Fourel, F., Simon, L., Lécuyer, C., 2020. Combined oxygen and sulphur isotope
485 analysis—a new tool to unravel vertebrate (paleo)-ecology. *Sci Nat* 107, 10. <https://doi.org/10.1007/s00114-019-1664-3>

486
487
488 Goedert, J., Lécuyer, C., Amiot, R., Arnaud-Godet, F., Wang, X., Cui, L., Cuny, G., Douay, G., Fourel, F., Panczer, G.,
489 Simon, L., Steyer, J.-S., Zhu, M., 2018. Euryhaline ecology of early tetrapods revealed by stable isotopes.
490 *Nature* 558, 68–72. <https://doi.org/10.1038/s41586-018-0159-2>

491 Gutiérrez, J.S., 2014. Living in Environments with Contrasting Salinities: A Review of Physiological and Behavioural
492 Responses in Waterbirds. *Arla* 61, 233–256. <https://doi.org/10.13157/arla.61.2.2014.233>

493 Hassler, A., Martin, J.E., Amiot, R., Tacail, T., Godet, F.A., Allain, R., Balter, V., 2018. Calcium isotopes offer clues on
494 resource partitioning among Cretaceous predatory dinosaurs. *Proceedings of the Royal Society B: Biological*
495 *Sciences* 285, 20180197. <https://doi.org/10.1098/rspb.2018.0197>

496 Hathorne, E.C., James, R.H., 2006. Temporal record of lithium in seawater: A tracer for silicate weathering? *Earth and*
497 *Planetary Science Letters* 246, 393–406. <https://doi.org/10.1016/j.epsl.2006.04.020>

498 Holt, E., Evans, J.A., Madgwick, R., 2021. Strontium (87Sr/86Sr) mapping: A critical review of methods and approaches.
499 *Earth-Science Reviews* 216, 103593. <https://doi.org/10.1016/j.earscirev.2021.103593>

500 Huh, Y., Chan, L.-H., Zhang, L., Edmond, J.M., 1998. Lithium and its isotopes in major world rivers: implications for
501 weathering and the oceanic budget. *Geochimica et Cosmochimica Acta* 62, 2039–2051.
502 [https://doi.org/10.1016/S0016-7037\(98\)00126-4](https://doi.org/10.1016/S0016-7037(98)00126-4)

503 Hussey, N.E., Kessel, S.T., Aarestrup, K., Cooke, S.J., Cowley, P.D., Fisk, A.T., Harcourt, R.G., Holland, K.N., Iverson,
504 S.J., Kocik, J.F., Mills Flemming, J.E., Whoriskey, F.G., 2015. Aquatic animal telemetry: A panoramic window
505 into the underwater world. *Science* 348, 1255642. <https://doi.org/10.1126/science.1255642>

506 James, R.H., Palmer, M.R., 2000. The lithium isotope composition of international rock standards. *Chemical Geology* 166,
507 319–326. [https://doi.org/10.1016/S0009-2541\(99\)00217-X](https://doi.org/10.1016/S0009-2541(99)00217-X)

508 Jones, C.M., 2006. Estuarine and Diadromous Fish Metapopulations, in: *Marine Metapopulations*. Academic Press.

509 Kocsis, L., Ősi, A., Vennemann, T., Trueman, C.N., Palmer, M.R., 2009. Geochemical study of vertebrate fossils from the
510 Upper Cretaceous (Santonian) Csehbánya Formation (Hungary): Evidence for a freshwater habitat of
511 mosasaurs and pycnodont fish. *Palaeogeography, Palaeoclimatology, Palaeoecology* 280, 532–542.
512 <https://doi.org/10.1016/j.palaeo.2009.07.009>

513 Lazzerini, N., Balter, V., Coulon, A., Tacail, T., Marchina, C., Lemoine, M., Bayarkhuu, N., Turbat, T., Lepetz, S., Zazzo,
514 A., 2021. Monthly mobility inferred from isoscapes and laser ablation strontium isotope ratios in caprine tooth
515 enamel. *Sci Rep* 11, 2277. <https://doi.org/10.1038/s41598-021-81923-z>

516 Lécuyer, C., 2016. Seawater residence times of some elements of geochemical interest and the salinity of the oceans.
517 *Bulletin de la Société Géologique de France* 187, 245–260. <https://doi.org/10.2113/gssgfbull.187.6.245>

518 Lécuyer, C., Goedert, J., Klee, J., Clauzel, T., Richardin, P., Fourel, F., Delgado-Darias, T., Alberto-Barroso, V., Velasco-
519 Vázquez, J., Betancort, J.F., Amiot, R., Maréchal, C., Flandrois, J.-P., 2021. Climatic change and diet of the
520 pre-Hispanic population of Gran Canaria (Canary Archipelago, Spain) during the Medieval Warm Period and
521 Little Ice Age. *Journal of Archaeological Science* 128, 105336. <https://doi.org/10.1016/j.jas.2021.105336>

522 Lugli, F., Cipriani, A., Capecechi, G., Ricci, S., Boschini, F., Boscato, P., Iacumin, P., Badino, F., Mannino, M.A., Talamo,
523 S., Richards, M.P., Benazzi, S., Ronchitelli, A., 2019. Strontium and stable isotope evidence of human mobility
524 strategies across the Last Glacial Maximum in southern Italy. *Nat Ecol Evol* 3, 905–911.
525 <https://doi.org/10.1038/s41559-019-0900-8>

526 Maxwell, S.L., 2007. Hydroacoustics: Rivers, in: *Salmonid Field Protocols Handbook: Techniques for Assessing Status*
527 *and Trends in Salmon and Trout Populations*.

528 Mesiar, D.C., Eggers, D.M., Gaudet, D.M., 1990. Development of techniques for the application of hydroacoustics to
529 counting migratory fish in large river. *Developments in Fisheries Acoustics* 189, 223–232.

530 Millot, R., Guerrot, C., Vigier, N., 2004. Accurate and High-Precision Measurement of Lithium Isotopes in Two Reference
531 Materials by MC-ICP-MS. *Geostandards and Geoanalytical Research* 28, 153–159.
532 <https://doi.org/10.1111/j.1751-908X.2004.tb01052.x>

533 Misra, S., Froelich, P.N., 2012. Lithium Isotope History of Cenozoic Seawater: Changes in Silicate Weathering and
534 Reverse Weathering. *Science* 335, 818–823. <https://doi.org/10.1126/science.1214697>

535 Penniston-Dorland, S., Liu, X.-M., Rudnick, R.L., 2017. Lithium isotope geochemistry. *Reviews in Mineralogy and*
536 *Geochemistry* 82, 165–217. <https://doi.org/10.1515/9783110545630-007>

537 Pimiento, C., Ehret, D.J., MacFadden, B.J., Hubbell, G., 2010. Ancient Nursery Area for the Extinct Giant Shark
538 Megalodon from the Miocene of Panama. *PLOS ONE* 5, e10552. <https://doi.org/10.1371/journal.pone.0010552>

539 Pimiento, C., MacFadden, B.J., Clements, C.F., Varela, S., Jaramillo, C., Velez-Juarbe, J., Silliman, B.R., 2016.
540 Geographical distribution patterns of Carcharocles megalodon over time reveal clues about extinction
541 mechanisms. *Journal of Biogeography* 43, 1645–1655. <https://doi.org/10.1111/jbi.12754>

542 Poet, M., Vigier, N., Bouret, Y., Jarretou, G., Bendahhou, S., Montanes, M., Thibon, F., Lasseur, R., Balter, V., Counillon,
543 L., submitted to eLife. Biological fractionation of lithium isotopes by cellular Na⁺/H⁺ exchangers unravels
544 fundamental transport mechanisms.

545 Pyenson, N.D., Kelley, N.P., Parham, J.F., 2014. Marine tetrapod macroevolution: Physical and biological drivers on
546 250Ma of invasions and evolution in ocean ecosystems. *Palaeogeography, Palaeoclimatology, Palaeoecology*,
547 Physical drivers in the evolution of marine tetrapods 400, 1–8. <https://doi.org/10.1016/j.palaeo.2014.02.018>

548 Quinn, T.P., 2018. *The Behavior and Ecology of Pacific Salmon and Trout*. University of Washington Press.

549 R Core Team, 2017. *R: A language and environment for statistical computing*. R Foundation for Statistical Computing,
550 Vienna, Austria.

551 Rempe, S.B., Pratt, L.R., Hummer, G., Kress, J.D., Martin, R.L., Redondo, A., 2018. The hydration number of Na⁺ in liquid
552 water. *Los Alamos National Laboratory publications*.

553 Rudolph, W., Brooker, M.H., Pye, C.C., 1995. Hydration of Lithium Ion in Aqueous Solutions. *J. Phys. Chem.* 99, 3793–
554 3797. <https://doi.org/10.1021/j100011a055>

555 Schmitz, B., Ingram, S.L., Dockery, D.T., Åberg, G., 1997. Testing ⁸⁷Sr/⁸⁶Sr as a paleosalinity indicator on mixed marine,
556 brackish-water and terrestrial vertebrate skeletal apatite in late Paleocene-early Eocene near-coastal
557 sediments, Mississippi. *Chemical Geology* 140, 275–287. [https://doi.org/10.1016/S0009-2541\(97\)00023-5](https://doi.org/10.1016/S0009-2541(97)00023-5)

558 Schultz, O., Bellwood, D.R., 2004. Trigonodon oweni and Asima jugleri are different parts of the same species Trigonodon
559 jugleri, a Chiseltooth Wrasse for the Lower and Middle Miocene in Central Europe (Osteichthyes, Labridae,
560 Trigonodontinae). *Annalen des Naturhistorischen Museums in Wien Serie A* 105, 287–305.

561 Séon, N., Amiot, R., Martin, J., Young, M., Middleton, H., Fourel, F., Picot, L., Valentin, X., Lécuyer, C., 2020.
562 Thermophysiology of Jurassic marine crocodylomorphs inferred from the oxygen isotope composition of their
563 tooth apatite. *Philosophical Transactions of the Royal Society B: Biological Sciences* 375, 20190139.
564 <https://doi.org/10.1098/rstb.2019.0139>

565 Skomal, G.B., Braun, C.D., Chisholm, J.H., Thorrold, S.R., 2017. Movements of the white shark *Carcharodon carcharias*
566 in the North Atlantic Ocean. *Marine Ecology Progress Series* 580, 1–16. <https://doi.org/10.3354/meps12306>

567 Suarez, C., Gelfo, J.N., Moreno-Bernal, J.W., Velez-Juarbe, J., 2021. An early Miocene manatee from Colombia and the
568 initial Sirenian invasion of freshwater ecosystems. *Journal of South American Earth Sciences* 109, 103277.
569 <https://doi.org/10.1016/j.jsames.2021.103277>

570 Thibon, F., Metian, M., Oberhänsli, F., Montanes, M., Vassileva, E., Orani, A.M., Telouk, P., Swarzenski, P., Vigier, N.,
571 2021. Bioaccumulation of Lithium Isotopes in Mussel Soft Tissues and Implications for Coastal Environments.
572 *ACS Earth Space Chem.* <https://doi.org/10.1021/acsearthspacechem.1c00045>

573 Thibon, Fanny, Weppe, L., Montanes, M., Telouk, P., Vigier, N., 2021. Lithium isotopic composition of reference materials
574 of biological origin TORT-2, DORM-2, TORT-3, DORM-4, SRM-1400 and ERM-CE278k. *J. Anal. At. Spectrom.*
575 36, 1381–1388. <https://doi.org/10.1039/D1JA00045D>

576 Thibon, F., Weppe, L., Vigier, N., Churlaud, C., Lacoue-Labarthe, T., Metian, M., Cherel, Y., Bustamante, P., 2020. Large-
577 scale survey of lithium concentrations in marine organisms. *Science of The Total Environment* 751, 1453.
578 <https://doi.org/10.1016/j.scitotenv.2020.141453>

579 Uhen, M.D., 2007. Evolution of marine mammals: Back to the sea after 300 million years. *The Anatomical Record* 290,
580 514–522. <https://doi.org/10.1002/ar.20545>

581 Vigier, N., Gislason, S.R., Burton, K.W., Millot, R., Mokadem, F., 2009. The relationship between riverine lithium isotope
582 composition and silicate weathering rates in Iceland. *Earth and Planetary Science Letters* 287, 434–441.
583 <https://doi.org/10.1016/j.epsl.2009.08.026>

584 Wißing, C., Rougier, H., Baumann, C., Comeyne, A., Crevecoeur, I., Drucker, D.G., Gaudzinski-Windheuser, S.,
585 Germonpré, M., Gómez-Olivencia, A., Krause, J., Matthies, T., Naito, Y.I., Posth, C., Semal, P., Street, M.,
586 Bocherens, H., 2019. Stable isotopes reveal patterns of diet and mobility in the last Neandertals and first
587 modern humans in Europe. *Sci Rep* 9, 4433. <https://doi.org/10.1038/s41598-019-41033-3>

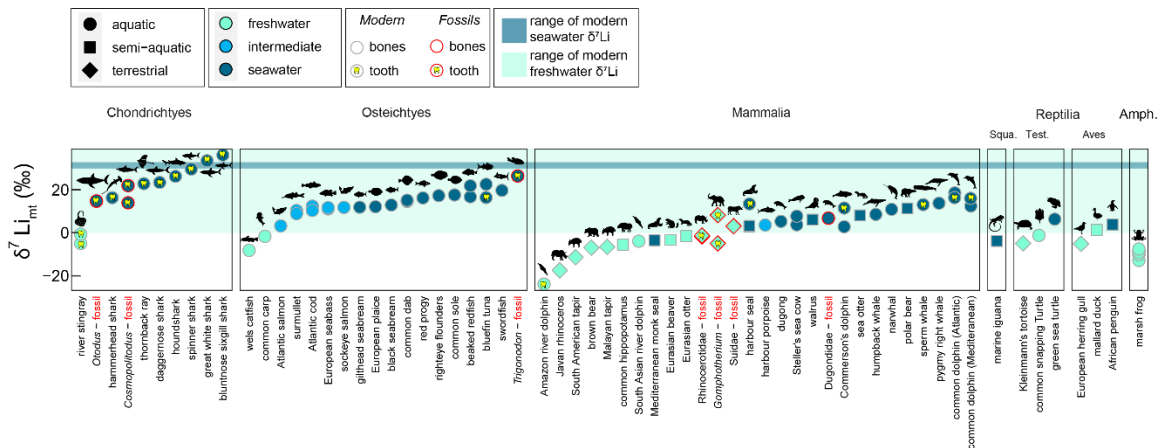
588 Zazzo, A., Lécuyer, C., Sheppard, S.M.F., Grandjean, P., Mariotti, A., 2004. Diagenesis and the reconstruction of
589 paleoenvironments: A method to restore original $\delta^{18}\text{O}$ values of carbonate and phosphate from fossil tooth
590 enamel. *Geochimica et Cosmochimica Acta* 68, 2245–2258. <https://doi.org/10.1016/j.gca.2003.11.009>

591
592

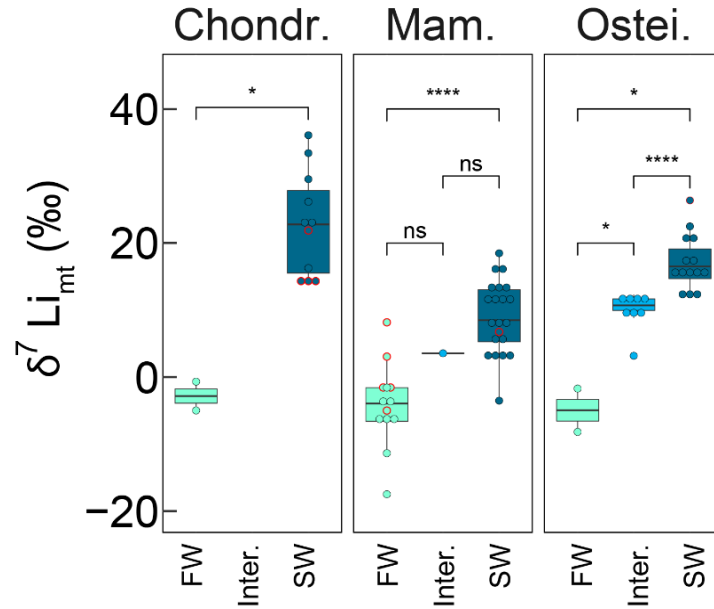
593 **Figures and Tables**

594

595

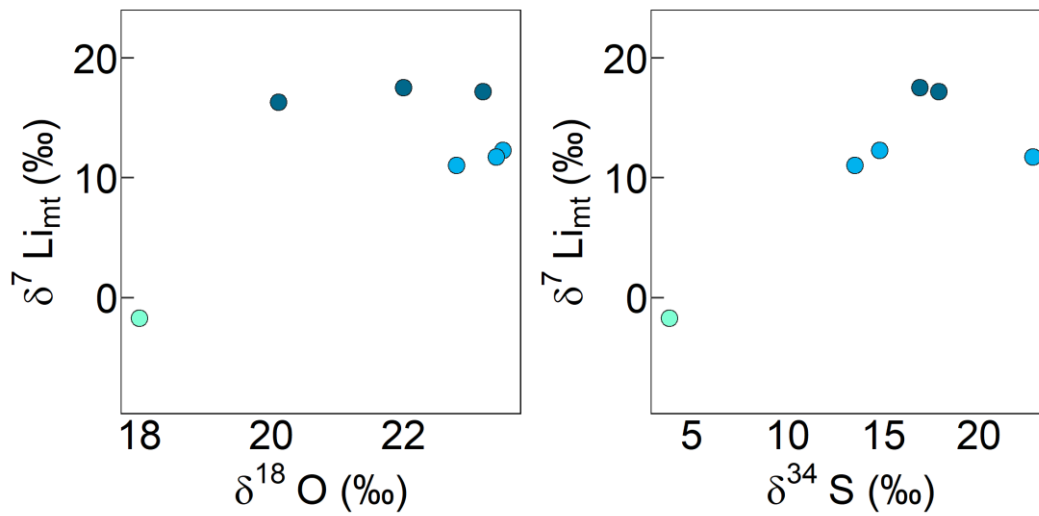


596 **Figure 1. $\delta^7\text{Li}_{\text{mt}}$ values of modern and fossil vertebrates including Chondrichthyes,**
 597 **Osteichthyes, Mammalia, Reptilia, and Amphibia.** Each icon represents an independent
 598 individual, except when tooth and bone from the same individual were sampled. Squa. for
 599 Squamata, Test. for Testudinea, Amph. for Amphibia. Vertebrates living in seawater have, on
 600 average, higher $\delta^7\text{Li}_{\text{mt}}$ values than those living in intermediate environments, which in turn display
 601 higher $\delta^7\text{Li}_{\text{mt}}$ values than vertebrates depending on freshwater. SD are included in the size of the
 602 markers.



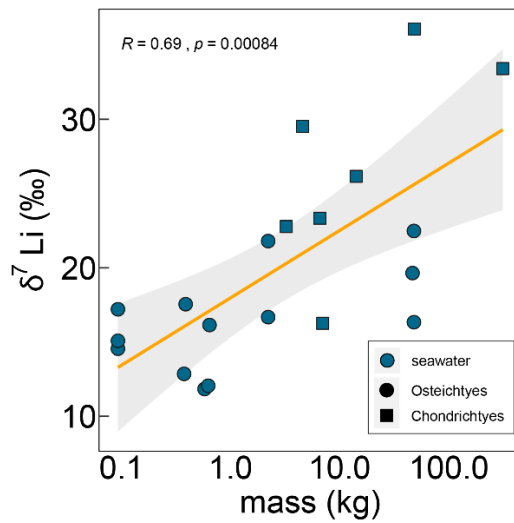
603

604 **Figure 2. Distinction of water environments based on $\delta^7\text{Li}_{\text{mt}}$ values.** Boxplot showing
 605 Chondrichthyes, Mammalia, and Osteichthyes $\delta^7\text{Li}_{\text{mt}}$ values according to their habitat (FW for
 606 freshwater, Inter. for intermediate water, and SW for seawater). Individual icons are added on top
 607 of each boxplot. Circles with red contours are fossil samples. Asterisks indicate p -values from the
 608 Mann-Whitney-Wilcoxon test (see Method section for details) and highlight the significance of the
 609 observed differences between pairs of groups: ns (not significant) for $p > 0.05$, * for $p < 0.05$, **
 610 for $p < 0.01$, *** for $p < 0.001$, **** for $p < 0.0001$. Chondrichthyes and Mammalia living in
 611 seawater have statistically higher $\delta^7\text{Li}_{\text{mt}}$ values than those living in freshwater environments. For
 612 Osteichthyes, species depending on intermediate environments have intermediate – and
 613 statistically different – $\delta^7\text{Li}_{\text{mt}}$ values between the ones for seawater and freshwater species.



614

615 **Figure 3. Modern Osteichthyes $\delta^7\text{Li}_{\text{mt}}$ values** compared to their corresponding (A) $\delta^{18}\text{O}$ values
 616 and (B) $\delta^{34}\text{S}$ values. $\delta^{34}\text{S}$ and $\delta^{18}\text{O}$ values are from Goedert et al. (Goedert et al., 2020). See Fig.
 617 1 for color legend. In contrast with $\delta^{34}\text{S}$ and $\delta^{18}\text{O}$ values, $\delta^7\text{Li}_{\text{mt}}$ values alone can discriminate
 618 between fish living in seawater and intermediate environments.



619

620 **Figure 4. $\delta^7\text{Li}_{\text{mt}}$ values vs individual body mass for modern Chondrichthyes and**
 621 **Osteichthyes.** The orange line is the linear regression line (regression coefficient $r^2=0.47$), and
 622 the surrounding grey area is the 95 % confidence interval. R is the Pearson correlation
 623 coefficient. A strong and positive correlation exists between $\delta^7\text{Li}_{\text{mt}}$ values and individual body
 624 mass.

			n	$\delta^7\text{Li}_{\text{mt}}$ (‰)				Li_{mt} (µg/g)			
				min	max	mean	SD	min	max	mean	SD
Chondrichthyes	seawater	modern	7	16.3	36.0	26.8	6.8	1.1	3.1	2.0	0.7
		fossil	4	13.9	21.9	16.3	3.7	3.0	4.9	4.1	0.9
	freshwater	modern	2	-5.0	-0.7	-2.8	3.1	0.2	0.5	0.4	0.3
Osteichthyes	seawater	modern	13	11.8	22.5	16.5	1.3	0.7	4.0	2.0	0.9
		fossil	1			26.4				6.9	
	freshwater	modern	2	-8.2	-1.7	-5.0	4.6	0.2	0.6	0.4	0.2
Mammalia	seawater	modern	20	-3.5	18.5	9.1	5.6	0.2	2.3	1.0	0.5
		fossil	1			6.7				1.8	
	freshwater	modern	9	-23.9	-1.5	-8.9	7.4	0.1	1.2	0.6	0.3
		fossil	5	-5.0	8.1	0.6	5.1	2.5	19.0	7.8	6.6
Reptilia	seawater	modern	3	-3.8	6.3	2.1	5.3	0.7	1.2	0.9	0.3
	freshwater	modern	4	-5.1	1.3	-2.5	3.1	0.5	2.2	1.0	0.8
Amphibia	freshwater	modern	5	-12.8	-7.6	-9.6	2.1	0.4	0.5	0.5	0.1

625

626 **Table 1. $\delta^7\text{Li}_{\text{mt}}$ values and Li_{mt} concentrations of modern and fossil vertebrates including**

627 **Chondrichthyes, Osteichthyes, Mammalia, Reptilia, and Amphibia.** “n” represents the

628 number of samples analysed, “min” the minimum value, “max” the maximum value, “mean” the

629 average value, and “SD” the standard deviation.

630